Properties of Bio-based Gum Arabic/Clay Aerogels

Liang Wang, Miguel Sánchez-Soto* and Tobias Abt

Centre Catalá del Plástic. Universitat Politécnica de Catalunya, Barcelona Tech. C/Colom 114, 08222, Terrassa, Spain.

Correspondence to: Miguel Sánchez-Soto (E-mail: m-sanchez-soto@upc.edu),Tel: (+0034) 937837022. Fax: (+0034) 937841827.

Abstract

Lightweight bio-based aerogels from sustainable gum Arabic (GA) and sodium montmorillonite (Na^+-MMT) clay were prepared by means of a simple freeze-drying process. GA/clay aerogels showed high porosity (87.9%-94.9%) of mainly open type and the mechanical properties were improved by the clay. When 40% of clay was added to pure GA, the specific modulus and the absorbed energy of resultant aerogels increased by 1.6 and 4.2 times respectively. On the other hand, the exponent value for modulus in the power-law model for cellular materials increased from 1.95 to 3.28 due to the more anisotropic structures induced by the presence of the clay. In terms of thermal stability and flame retardancy, clay content played a dominant role. With 50% of clay loading, the initial decomposition temperature increased by nearly 16 ^oC and the peak of heat release rate was 3-fold reduced.

Keywords: Gum Arabic; Aerogels; Clay; Porosity; Flame retardancy; Thermal stability.

1. Introduction

Increasing concern on environmental protection requires the limitation of usage of petroleum-based synthetic plastics and the development of new ecological solutions to

replace them in order to reduce pollution, wastes and green-house gases. Foams are one of the common forms for polymers with applications including thermal insulation, packaging or cushioning to mention a few (Oertel, 1994). The majority of the low-density foams existing in the market are derived from petroleum and are not biodegradable. Therefore, alternatives based on polymers derived from renewable resources (bio-based polymers) are attracting an increasing attention. Among the different bio-based polymers, namely polyesters, proteins and polysaccharides, the latter have a great potential to be transformed into aerogels, a porous, lightweight foam-like material (Mikkonen et al., 2013).

Plastic foams are formed by a solid matrix skeleton and a gaseous phase which is derived from a blowing agent, and where the foaming process is carried out by applying mechanical, physical or chemical procedures to the solid material. In contrast, aerogels are created when the liquid contained in a wet gel is replaced by air. Aerogels are mainly obtained through supercritical drying (SCD) and contain a network of interconnected mesopores (2-50 nm). Due to their high surface area, they are used as drug carrier, catalyst, adsorbent or in insulating applications. Garcia-González et al. (2011) summarized the fundamental processing parameters and methods for preparing different polysaccharide-based aerogels trough SCD, showing that polysaccharides can be used as an alternative to silica-based aerogels for drug delivery. Quignard et al. (2008) also employed this technique to prepare different marine polysaccharide aerogels for heterogeneous catalyst supports based on alginates, carrageenan and chitosan. Those aerogels presented a high specific surface area (200-570 m^2/g) and were stable in most organic solvents. Superabsorbent alginate aerogels were prepared by Mallepally et al. (2013). In their work, the aerogels were capable of absorbing about 120 times their weight in saline water in 24 hours. The observed behavior was attributed to the large pore volume and high specific surface area (~500 m^2/g) of the aerogels as well as the polymer increasing in charge in the presence of salt ions. Finally, Rudaz et al. (2014) reported the preparation of superinsulating mechanically strong aerogels from pectin having a thermal conductivity as low as 0.016-0.020 W/(m.K) which was attributed to the low density

(< 0.15 g/cm^3) and nanometric dimensions of pores, leading to a decrease of conduction in the gas phase.

In contrast to SCD, freeze-drying applied to polysaccharide solutions usually yields structures having micron-sized pores. The nucleation and ice growth destroy the gel network, creating large pores and thus having considerably lower specific surface area. The aerogel structure is the result of the ice sublimation and is composed of a solid phase and a large fraction of air, which correspond to the volumes occupied by the biopolymer and ice in the frozen gel, respectively. In this process, the water solubility, swelling and gel-forming capability of polysaccharides contribute to the stability of the so-formed aerogels (Quignard et al., 2008). Several polysaccharide-based aerogels have been prepared through freeze-drying. Sehaqui et al. (2010) produced high porosity foam-like materials based on cellulose nanofibers. Due to its high affinity with cellulose, xyloglucan was employed to increase the strength and stiffness of the resultant micro-porous aerogels. Bendahou et al. (2014) combined extracted cellulose, cellulose nanofibers and nanozeolite particles to create hybrid aerogel monoliths. The thermal conductivity of cellulose nanofibers aerogels was found to decrease with nanozeolite content whereas it remained almost constant in the case of extracted cellulose aerogels. This was attributed to the different microstructures and the embedment of nanozeolite in cellulose nanofibers. Valentin et al. (2003) compared SCD with freeze-drying in chitosan aerogels, finding that SCD yields considerably higher porosity although freeze-dried aerogels showed even lower density than the ones dried with supercritical carbon dioxide. In general, these open cell freeze-dried bio-aerogels exhibit the properties of the precursor polymer but usually have low Young's modulus and reduced load-bearing capacity. Nevertheless, different approaches such as crosslinking (Pojanavaraphan et al., 2010) or filler reinforcement (Svagan et al., 2008) can be followed to improve aerogel performance. Among these methods, clay addition has been proved to be an economic and straightforward way to enhance both the thermal and mechanical properties and to expand the range of its potential applications. Following this approach, Chen et al. (2012) used a combination of alginate and sodium montmorillonite clay to create low

flammability robust aerogels with mechanical properties close to that of balsa wood. Calcium cation crosslinking increased the solution viscosity leading to a finer network structure and to a further enhancement of mechanical properties. In another approach, xanthan gum /clay aerogels were produced by Wang et al. (2014). The increase of the content of xanthan gum lead to a network structure which increased the mechanical properties. However, a synergic effect was found by the introduction of agar. In the presence of both polysaccharides, the resultant aerogels displayed a significant improvement in mechanical properties as compared to those containing a single biopolymer. Chen et al. (2013a) combined clay and cation crosslinking to form pectin/clay aerogels with enhanced mechanical properties and thermal resistance. The introduction of clay generated a much rougher microstructure and also contributed to increase the decomposition temperature due to the themal insulation and mass-transport barrier created by the clay layers. Among the different polysaccharides, gum Arabic (GA) exhibits a very high solubility in water. Unlike other gums, GA can be dissolved even at high concentrations (up to 50% w/v) withouth showing a remarkable increase in viscosity. These characteristics make GA a very attractive precursor for producing GA/clay hybrid aerogels.

Gum Arabic is an exudate from the *Acacia* tree and its precise molecular structure is little known. It is recognized by many researchers that gum Arabic consists of a mixture of arabinogalactan polysaccharide (major component) and hydroxyproline protein (minor component) (Idris et al., 1998; Islam et al., 1997; Randall et al., 1988). The main structural feature of the major component is a β-(1→3)-galactose backbone and 1,6-linked galactose side chains terminating in β-D glucuronic acid. Moreover, the properties of GA differ according to the botanical source (Cozic et al., 2009). Due to its unique emulsification, film-forming, and encapsulation properties, GA is extensively used in industry, such as food (Krishnan et al., 2005), paper (Verbeken et al., 2003) and pharmacy (Ward, 2000).

In the current work, bio-based light-weight GA aerogels were prepared using an environmentally-friendly freeze-drying process with the aim of providing alternatives

to replace packaging materials traditionally prepared from non-biodegradable petrochemical products. Hybrid organic-inorganic aerogels were also created by adding sodium montmorillonite (Na^+-MMT) clay to GA aqueous solution. The resultant aerogel composites were expected to show improved thermal and mechanical properties than the neat GA aerogels. The microstructures, compression properties, thermal stability and flame retardancy of aerogels were investigated, respectively.

2. Material and Methods

2.1. Materials

Gum Arabic in powder form was bought from T3Q Quimica (Spain). Its physicochemical properties resulted from a preliminary characterization are reported in Table 1. Sodium Montmorillonite (Na^+-MMT, PGW grade) was purchased from Southern Clay (USA), having a density of 2.6 g/cm^3 and cation exchange capacity (CEC) of 145 meq/100 g. All materials were used as received.

2.2. Aerogel Preparation

GA aerogels: GA powder was dissolved in deionized (DI) water at room temperature under magnetically stirring until achieving transparent solutions with different concentrations (5 wt%, 7.5 wt%, 10 wt% and 15 wt%). Then they were poured into cylinder vials (diameter: 30mm) or square-shaped moulds (100 x 100 mm^2) before being frozen at -80ºC in an ethanol/solid CO_2 bath for 30 minutes. Aerogel samples were obtained after ice sublimation in a lyophilizer (Telstar Lyoquest) for 96 hours using a condenser temperature of -80 ^{o}C and vacuum of 0.01mbar.

GA/Clay aerogels: Clay suspensions were prepared by dispersing Na^+-MMT clay nanoparticles in DI water using an IKA Ultra-turrax disperser. GA solutions were obtained using the previously mentioned procedure. Then they were blended and mixed to attain homogenous precursor suspensions containing 5 wt% clay and various GA concentrations (5 wt%, 7.5 wt%, 10 wt%, 15 wt%). Finally, the same

freeze-drying process was applied to acquire GA/Clay aerogels.

Sample identification is GA or clay used followed by their respective concentration in precursor suspensions, i.e., GA5C5 represents a sample that was prepared from an aqueous suspension containing 5 wt% of gum Arabic and 5 wt% of clay.

2.3.Characterization

The sugar composition of the gum Arabic was determined by HPLC (Agilent 1100) using the procedure described by Randall et al. (1989). An ICSep ION-300 Interaction analysis column equipped with a refractive index detector was used. The sample (20 μdm^3) was injected into the column using 0.013M H_2SO_4 solution as eluent at flow rate of 0.4 cm^3/min. The retention times were monitored using a Beckman 156 refractive index detector. Individual standards of glucuronic acid, arabinose, galactose and rhamnose were used.

To determine the intrinsic viscosity of gum powder solutions the method of Solomon and Ciuta (1962) was used. Gum powder was dissolved in distilled water to a concentration of 0.01 g/cm^3 and analysed using a Cannon Ubbelohde size 75 viscosimeter with precise temperature control through a thermostatic bath at 25 ºC. Once the intrinsic viscosity was known, the molecular weight was calculated applying the Mark-Houwink-Sakurada equation:

$$[\eta] = k\,(M)^a \quad (1)$$

Where [η] is the intrinsic viscosity, M the molecular weight and k and a are the Mark-Houwink-Sakurada parameters.

The apparent density (ρ_{app}) of the aerogel samples was calculated from the mass and the actual specimen dimensions using a precision balance and a digital Vernier calliper, respectively. Five replicas were taken for each composition.

Theoretic densities (ρ_{ts}) of the GA/clay composite aerogels were calculated according to the equation:

$$\rho_{ts} = \frac{1}{w_{AG}/\rho_{AG} + w_C/\rho_C} \quad (2)$$

Where w_{GA} and w_C are the mass fractions of GA and clay in the dry aerogels, respectively ρ_{GA} and ρ_C are the densities of GA and clay, respectively. The clay density was 2.6 g/cm^3 according to the supplier; ρ_{GA} (1.302 ± 0.002g/cm^3) was determined using a helium pycnometer (Accupyc 1330) in which dried GA powder was tested.

The porosity (P) of the aerogel is defined as the volume fraction of voids and was calculated as follows:

$$P = \left(1 - \frac{\rho_{app}}{\rho_{ts}}\right) \times 100\% \quad (3)$$

A Jeol 5610 scanning electron microscope (Japan) operated at 10 kV was used to analyse the microstructures of the aerogels. The samples were cryofractured and coated with a gold layer prior to observation.

Compression testing was carried out along the vertical axis of the cylinder samples (main direction of ice growth) on a Galdabini (Italy) universal testing machine equipped with a load cell of 1kN following ISO 604 standard. The crosshead rate and maximum deformation were set to 1 mm/min and 70%, respectively. The Young's modulus and the absorbed energy were calculated from the experimental data. Three replicas of each sample were made.

TGA was carried out on a Mettler Toledo TGA/DSC1 equipment to study the thermal stability of the aerogels. Samples were loaded in alumina pans and heated at a rate of 10 ºC/min from 30 to 900 ºC under dry nitrogen.

The burning behavior of GA/clay aerogels were investigated using a cone calorimeter (Ineltec BECC model, Spain) following ISO 5660 standard. Square-cut samples (100 × 100 mm^2) with an average thickness of 7 mm were placed in a steel support and exposed to an external heat flux of 50 kW/m^2.

3. Results and Discussion

206 **3.1. Gum Arabic Preliminary Characterization.**

207 Table 1 shows the results of the preliminary characterization of the raw gum Arabic
208 powder including the determination of sugar content, intrinsic viscosity and molecular
209 weight. Data given by the supplier is also included. In a similar way like other gum
210 exudates from *Acacia* trees, the current one is rich in arabinose and galactose units
211 being rhamnose the minor component. The glucuronic acid was below the detection
212 limit of the equipment (< 3.5%). No other peaks than the ones under analysis
213 appeared, indicating the absence of other majoritarian components such us organic
214 acids or different monosaccharides. The constants of the Mark-Howing-Sakurada
215 equation were found to be K = 0,01311 cm^3/g and a = 0,5406 respectively (Masuelli,
216 2013). Accordingly, the resultant molecular weight was M=1,1 x 10^6 g/mol which is
217 consistent with data found in literature for *Acacia* senegal gums (Renard et al. 2006,
218 Randall et al. 1989).

219

220 Table 1. Physicochemical data and composition of gum Arabic powder

Physicochemical data	Value	Composition	Value
Moisture content (%)	7	Galactose (%)	39.8
Ash content (%)	3.4	Arabinose (%)	58,1
Optical rotation (degrees)	-25	Rhamnose (%)	2,1
pH (25% w, 20ºC)	4.1-4.8	Glucuronic acid (%)	-
Intrinsic viscosity (cm^3/g)	23.7	Molecular weight (g/mol)	$1,1x10^6$

221

222 **3.2. Density and Porosity**

223 The results of density and porosity of the samples are summarized in Table 2. Helium
224 is capable of penetrating into open pores of angstrom dimensions, giving the volume
225 occupied by open porosity (Chang, 1988). The skeletal density of sample GA10 was
226 measured using a helium pycnometer. Then the tested sample was ground to break the
227 closed-cell structure. The density of the ground sample was investigated in the same
228 manner. There was no difference between the two measurements, indicating the
229 absence of closed macro-pores in the aerogel. On the other hand, all tested samples

exhibited high porosities corresponding to the voids left by ice during its sublimation.

Table 2. Density and porosity of GA/clay aerogels

Samples	ρ_{app} (g/cm^3)	ρ_{ts} (g/cm^3)	Porosity (%)
GA7.5	0.085±0.001	1.302	93.5±0.1
GA10	0.109±0.018	1.302	91.6±1.4
GA15	0.154±0.009	1.302	88.2±0.1
GA5C5	0.088±0.001	1.735	94.9±0.1
GA7.5C5	0.115±0.001	1.623	92.9±0.1
GA10C5	0.149±0.013	1.562	90.5±0.1
GA15C5	0.180±0.002	1.488	87.9±0.1

For neat GA aerogels, increasing the GA content from 7.5 to 15 wt%, the porosity reduced by 5.3%. A similar tendency was observed when clay was added. As expected, a higher content of solid component led to a lower void fraction.

3.3. Morphology

Freeze drying of aqueous GA/clay gels produced stable aerogel monoliths retaining the shape of the used mould, as can be seen in Figure 1. Pure clay aerogels are capable to form stable three dimensional objects because the particles are linked edge-to-face creating a “house of cards” structure due the opposite surface and edge charges that exist in clays. However, this material is very brittle. The addition of a polymer yields a more robust material provided that the polymer covers the clay layers and bridges the gaps left by the ice after sublimation.

The morphological microstructures of GA/clay aerogels are shown in Figure 2. Sample GA7.5 exhibited a layered structure without polymer struts between layers (Figure 2a). When the content of GA was increased to 15 wt%, the layers increased in thickness. However, there was no apparent change in the number of polymeric struts connecting the clay layers (Figure 2b). Compared to other biopolymer aerogels, for example xanthan gum (Wang et al., 2014), GA aerogels prepared from precursor solutions having a high concentration (15 wt%) did not display network structures.

The reason is that GA solutions retain a low viscosity even at high concentration. For instance, 30% GA solutions have a lower viscosity than 1% xanthan gum at low shear rates (Phillips and Williams, 2009).

When 5wt% of clay was added to the precursor solution of GA7.5, its viscosity was increased. The ice front growth was retarded by the higher fluid viscosity and secondary crystallization occurred (Deville et al., 2006), meaning that ice nucleation and growth occurred in a direction different from the main one (vertical). As a result, smaller ice crystals were generated, resulting in a rough fracture surface (Figure 2c). Increasing the GA concentration in the precursor suspension of GA/clay aerogels (sample GA15C5), a continuous "house of cards" structure (Figure 2d) appeared due to the further increment of viscosity.

These different aerogel microstructures are responsible for the mechanical property changes discussed in the following section.

3.4. Compressive Properties

The compressive stress-strain curves of the GA and GA/clay aerogels are shown in Figure 3. Generally, these samples showed a compressive behaviour similar to the one of elastic-plastic polymeric foams. Compressive mechanical properties, such as compressive modulus (E), specific compressive modulus (E_s), compressive stress at 70% strain (σ_{max}), and absorbed energy (E_a) are listed in Table 3. It should be mentioned that the sample GA5 was too brittle to be tested.

Regarding neat GA aerogels, increasing the polymer content, σ_{max} and E_a of the samples increased. However, there was no significant change in specific compressive modulus (E_s). This is because the density of polymeric struts between the layers in the aerogels did not increase with GA content, as shown in the SEM observations.

When 5wt% of clay was added, the specific modulus of GA7.5C5 increased by 1.6 times compared to GA7.5 (see Table 3). This result was consistent with the finding in prior works on biopolymer-clay aerogel composites (Chen et al., 2013a; Chen et al., 2013b). Sample GA15C5 showed a layered structure with denser polymer

283 struts (Figure 2d) as compared to GA7.5C5, thus it exhibited a more robust structure
284 and better mechanical properties. However, both GA and clay platelet surface are
285 negatively charged and thus a weak adhesion is produced between them, resulting in
286 the appearance of small fractures that can be observed as kinks in the compressive
287 pattern of sample GA15C5 in Figure 3.
288
289 Table 3. Compressive mechanical properties of GA/clay aerogels

Samples	E (MPa)	E_s (MPa/g cm^3)	σ_{max}(MPa)	E_a (kJ/cm^3)
GA7.5	0.6±0.1	7.5±2.1	-	12±2
GA10	1.4±0.3	10.6±2.1	0.25±0.1	49±12
GA15	2.1±0.7	10.9±2.9	1.10±0.1	240±45
GA5C5	1.2±0.2	13.9±2.0	0.35±0.1	44±3
GA7.5C5	2.3±0.1	19.4±1.1	0.40±0.1	62±15
GA10C5	4.0±0.6	30.0±3.4	0.60±0.2	70±1
GA15C5	25.8±4.2	143 ±23	1.30±0.1	315±20

290
291 The addition of clay reinforced the mechanical properties of the aerogels. The
292 power-law developed by Gibson and Ashby (Gibson and Ashby, 1999) for cellular
293 solids was used to analyse mechanical properties:
294
$$K/K_S \propto C\left(\rho/\rho_S\right)^n \quad (3)$$

295 Where K means a mechanical property of foams, K_S is the property of the
296 corresponding fully solid material. ρ and ρ_s are the apparent density and skeletal
297 density, respectively; ρ_s herein is thought to be equal to the theoretical skeletal density.
298 C and n are structural parameters (Gibson and Ashby, 1999; Hilyard, 1982). In present
299 work, exponent values for modulus and ultimate strength of GA aerogels were 1.95
300 and 3.84, respectively. However, for GA/clay aerogel composites of which the relative
301 density (ρ/ρ_s) changed, the values of n were 3.53 and 1.46 for modulus and ultimate
302 strength, respectively.
303 The exponent values changed with the material structures. For open-cell foams,
304 the exponent was expected to be 2. Wood has an exponent of 3 in the radial direction
305 due to anisotropy of the structure (Gibson and Ashby, 1999) and silica aerogels show
306 a value in the range of 2.6-3.8 due to different sample preparation methods (Ma et al.,

2000). For pure GA aerogels, the exponent for modulus was 1.95 (Figure 4), which was similar to the one for aerocellulose (n=1.7) found by Sescousse et al. (2011) and was also consistent with the open structure generated in the aerogels. This value increased to 3.28 with the addition of clay, similar to the one found in PVOH-clay aerogels (3.74) by Alhassan et al. (2010). It was attributed to the reinforcing effect of clay and the more anisotropic structures induced by clay addition in the composites. Nevertheless, due to the scarce number of data, more experimental analyses on the mechanical properties of this type of aerogels are needed to confirm the results.

3.5. Thermal Stability

Thermal stability of GA/clay aerogels were studied using thermogravimetric analysis under dry nitrogen atmosphere. The weight loss curves are shown in Figure 5. The decomposition of aerogels can be divided into three stages. The moisture in GA-based aerogels was firstly evaporated under the thermal loading up to 150 ^{o}C. Then dehydration and decarboxylation reactions of GA occurred when the temperature was over 250^{o}C until the formation of char (~330 ^{o}C) (Cozic et al., 2009). Finally, with increasing temperature, the char was slowly oxidized to yield aromatic components. $T_{d5\%}$ is defined as the temperature at which 5% weight loss occurred after 150 ^{o}C (dW/dT≈0). It was recorded as the initial decomposition temperature of the aerogels. Table 4 summarizes the temperatures at 5% weight loss ($T_{d5\%}$), temperatures at maximum weight loss rate (T_{dmax}), maximum weight loss rates (dW/dT_{max}) and residue amounts (W_R).

In comparison to sample GA5, it can be observed that GA5C5 presented a higher $T_{d5\%}$ (275 ^{o}C) and a much lower maximum weight loss rate (0.7 %/^{o}C). The clay nanoplatelets acted as a physical barrier, enhancing the heat resistance of materials (Rao and Pochan, 2007). Regarding sample GA15C5, $T_{d5\%}$ increased by nearly 7 ^{o}C and the maximum weight loss rate decreased by 0.4 %/^{o}C as compared to GA15, respectively. The differences in thermal stability of the samples GA5C5 and GA15C5

were attributed to the relative clay content in the composites. A higher clay content led to a lower degradation rate and a higher initial decomposition temperature. This is due to the formation of a denser clay layer char, as can be observed from the difference in their residue amounts. However, clay addition caused a lower T_{dmax}, possibly related to the higher thermal conductivity that is resulted from a denser and more compact structure of the aerogel.

Table 4. Parameters for thermal stability of GA/clay aerogels

Samples	$T_{d\,5\%}$ (°C)	$T_{d\,max}$ (°C)	dW/dT_{max}(%/°C)	Residue (%)
GA5	258.6	310.4	1.41	13.2
GA5C5	274.5	299.0	0.69	52.3
GA15	261.2	311.7	1.47	16.5
GA15C5	267.7	308.3	1.09	38.2

3.6. Combustion Behavior

The combustion behavior of the aerogels was investigated using cone calorimetry. The resultant heat released during burning is determined in terms of heat release rate (HRR) as a function of burning time, as seen in Figure 6. The detailed flammability parameters, such as time to ignition (t_i), time to flame extinguish (t_e), peak of heat release rate (PHRR), total heat release (THR), time to peak of heat release rate (TTPHRR), and fire growth rate (FGR), are given in Table 5. A double peak signal appeared in the HRR curves of the sample loaded with clay. It seemed to be due to the transient protective effect of the clay layers during the combustion (Alexandre and Dubois, 2000). The combustion of the rest of material occurred when the layer was broken.

The time to ignition was similar in all cases and corresponded to the time for generating the critical amount of combustible gas in the gas phase. Sample GA15 had a PHRR value of 233kW/m^2 and time to PHRR of 36 s. Adding 33% of clay, PHRR decreased to 121 kW/m^2 and the FGR values reduced from 6.5 to 4.5kWm^{-2}s, indicating a lower rate of combustion. This tendency was also found for the other bio-based aerogels when clay was used to improve the flame retardant properties

(Wang et al., 2014).This is due to the clay enrichment on the sample surface during the increasing thermal load (Kashiwagi et al., 2004), which brings a decomposition rate decrease for the underlying polymer fraction. Moreover, the presence of clay and its characteristic structural network forms a complex labyrinth through which combustion gases diffuse out of the material (Chen et al., 2012). Decreasing the amount of polymer in the GA/clay aerogels, the flame retardant effect of clay was more remarkable, as displayed in sample GA5C5.

Table 5. Combustive parameters of GA/clay aerogels

Samples	t_i (s)	t_e (s)	TTHRR (s)	PHRR (kW/m^2)	FGR (kW/m^2 s)	THR (MJ/m^2)	Residue (%)
GA15	10	386	36	232.9	6.5	19	2.9
GA15C5	11	146	27	121.1	4.5	17.2	23.6
GA5C5	15	91	24	56.4	2.4	4.9	45.4

4. Conclusions

Gum arabic, a type of polysaccharide from African plants, was used to prepare “green” aerogels. Clay was added to form GA/clay aerogel composites. GA-based aerogels had a typical lamellar structure created by the ice template. Neat GA aerogels behaved in a brittle manner due to insufficient polymer connection between layers. With the addition of clay, the compressive mechanical properties were markedly improved. The thermal stability and flame retardant properties were found to be dependent on clay content in the aerogel composites. Clay layers formed during the burning process and acted as a physical barrier, protecting the sample underneath.

Acknowledgements

Authors acknowledge the financial support of this work given by the Spanish Government through the projects MAT 2013-40730-P. Also Liang Wang thanks the China Scholarship Council for the grant received.

References

Alexandre, M., Dubois, P., 2000. Polymer-layered silicate nanocomposites: preparation, properties and uses of a new class of materials. Materials Science and Engineering: R: Reports 28, 1-63.

Alhassan, S.M., Qutubuddin, S., Schiraldi, D., 2010. Influence of Electrolyte and Polymer Loadings on Mechanical Properties of Clay Aerogels. Langmuir 26, 12198-12202.

Bendahou, D., Bendahou, A., Seantier, B., Grohens, Y., Kaddami, H., 2014. Nano-fibrillated cellulose-zeolites based new hybrid composites aerogels with super thermal insulating properties. Industrial Crops and Products 65, 374-382.

Chang, C., 1988. Measuring density and porosity of grain kernels using a gas pycnometer. Cereal Chem 65, 13-15.

Chen, H.-B., Chiou, B.-S., Wang, Y.-Z., Schiraldi, D.A., 2013a. Biodegradable Pectin/Clay Aerogels. ACS applied materials & interfaces 5, 1715-1721.

Chen, H.-B., Wang, Y.-Z., Sánchez-Soto, M., Schiraldi, D.A., 2012. Low flammability, foam-like materials based on ammonium alginate and sodium montmorillonite clay. Polymer 53, 5825-5831.

Chen, H.-B., Wang, Y.-Z., Schiraldi, D.A., 2013b. Foam-like materials based on whey protein isolate. European polymer journal 49, 3387-3391.

Cozic, C., Picton, L., Garda, M.-R., Marlhoux, F., Le Cerf, D., 2009. Analysis of gum arabic: Study of degradation and water desorption processes. Food Hydrocolloids 23, 1930-1934.

Deville, S., Saiz, E., Nalla, R.K., Tomsia, A.P., 2006. Freezing as a path to build complex composites. Science 311, 515-518.

García-González, C., Alnaief, M., Smirnova, I., 2011. Polysaccharide-based aerogels-Promising biodegradable carriers for drug delivery systems. Carbohydrate Polymers 86, 1425-1438.

Gibson, L.J., Ashby, M.F., 1999. Cellular solids: structure and properties, 2nd Ed. Cambridge university press. Cambridge.

Hilyard, N., 1982. Mechanics of cellular plastics. Ed. Macmillan. New York.

Idris, O., Williams, P., Phillips, G., 1998. Characterisation of gum from Acacia senegal trees of different age and location using multidetection gel permeation chromatography. Food Hydrocolloids 12, 379-388.

Islam, A., Phillips, G., Sljivo, A., Snowden, M., Williams, P., 1997. A review of recent developments on the regulatory, structural and functional aspects of gum arabic. Food Hydrocolloids 11, 493-505.

Kashiwagi, T., Harris Jr, R.H., Zhang, X., Briber, R., Cipriano, B.H., Raghavan, S.R., Awad, W.H., Shields, J.R., 2004. Flame retardant mechanism of polyamide 6-clay nanocomposites. Polymer 45, 881-891.

Krishnan, S., Kshirsagar, A.C., Singhal, R.S., 2005. The use of gum arabic and modified starch in the microencapsulation of a food flavoring agent. Carbohydrate Polymers 62, 309-315.

Ma, H.-S., Roberts, A.P., Prévost, J.-H., Jullien, R., Scherer, G.W., 2000. Mechanical structure-property relationship of aerogels. Journal of Non-Crystalline Solids 277, 127-141.

Mallepally, R.R, Bernard, I, Marin, M.A., Ward, K.A., McHugh, M.A., 2013. Superabsorbent alginate aerogels. The Journal of Supercritical Fluids 79, 202-208.

Masuelli, M.A., 2013. Hydrodinamic properties of whole Arabic gum. American Journal of Food

Science and Technology 1, 60-66.
Mikkonen, K.S., Parikka, K., Ghafar, A., Tenkanen, M., 2013. Prospects of polysaccharide aerogels as modern advanced food materials. Trends in Food Science & Technology 34, 124-136.
Oertel, G., 1994. Polyurethane handbook. 2nd Ed. Hanser. Munich.
Phillips, G.O., Williams, P.A., 2009. Handbook of hydrocolloids. 2nd Ed. Woodhead. Cambridge.
Pojanavaraphan, T., Magaraphan, R., Chiou, B.-S., Schiraldi, D.A., 2010. Development of biodegradable foamlike materials based on casein and sodium montmorillonite clay. Biomacromolecules 11, 2640-2646.
Quignard, F., Valentin, R., Di Renzo, F., 2008. Aerogel materials from marine polysaccharides. New Journal of Chemistry 32, 1300-1310.
Randall, R. C., Phillips, G. O., Williams, P. A., 1988. The role of the proteinaceous component on the emulsifying properties of gum arabic. Food Hydrocolloids 2, 131-140.
Randall, R.C., Phillips, G. O., Williams, P. A., 1989. Fractionation and characterization of gum from *Acacia senegal*. Food Hydrocolloids 3, 65-75.
Renard, D., Lavenant-Gourgeon , L., Ralet, M.C., Sanchez, C., 2006. Acacia senegal gum: continuum of molecular species differing by their protein to sugar ratio, molecular weight, and charges. Biomacromolecules 7, 2637-2649.
Rao, Y., Pochan, J.M., 2007. Mechanics of polymer-clay nanocomposites. Macromolecules 40, 290-296.
Rudaz, C., Courson, R., Bonnet, L., Calas-Etienne, S., Sallée, H., Budtova, T., 2014. Aeropectin: Fully biomass-based mechanically strong and thermal superinsulating aerogel. Biomacromolecules 15, 2188-2195.
Sescousse, R., Gavillon, R., Budtova, T., 2011. Aerocellulose from cellulose-ionic liquid solutions: Preparation, properties and comparison with cellulose-NaOH and cellulose-NMMO routes. Carbohydrate polymers 83, 1766-1774.
Solomon, O.F., Ciuta, I. Z., 1962. Détermination de la viscosité intrisiqué de solutions de polymères par une simple détermination de la viscosité. Journal of Applied Polymer Science 6, 683-686.
Sehaqui, H., Salajkov, M., Zhou, Q., Berglund, L.A., 2010. Mechanical performance tailoring of tough ultra-high porosity foams prepared from cellulose I nanofiber suspensions. Soft Matter 6, 1824-1832.
Svagan, A.J., Samir, M.A., Berglund, L.A., 2008. Biomimetic foams of high mechanical performance based on nanostructured cell walls reinforced by native cellulose nanofibrils. Advanced Materials 20, 1263-1269.
Valentin, R., Molvinger, K., Quignard, F., Brunel, D., 2003. Supercritical CO_2 dried chitosan: an efficient intrinsic heterogeneous catalyst in fine chemistry. New Journal of Chemistry 27, 1690-1692.
Verbeken, D., Dierckx, S., Dewettinck, K., 2003. Exudate gums: occurrence, production, and applications. Applied Microbiology and Biotechnology 63, 10-21.
Wang, L., Schiraldi, D.A., Sanchez-Soto, M., 2014. Foam-like Xanthan gum/clay Aerogel Composites and Tailoring Properties by Blending with Agar. Industrial & Engineering Chemistry Research 53 7680-7687.
Ward, F.M., 2000. Uses of gum arabic (Acacia sp.) in the food and pharmaceutical industries, Cell and Developmental Biology of Arabinogalactan-Proteins. Springer, 231-239.

Figure Caption:

Figure 1. Photograph showing samples after freeze-drying: (a) pure GA aerogels; (b) GA/clay aerogels.

Figure 2. SEM photos of GA/clay aerogels: (a) GA7.5; (b) GA15; (c) GA7.5C5; (d) GA15C5.

Figure 3. Compressive curves of GA/clay aerogels.

Figure 4. Compressive modulus of the aerogels as function of relative density. Insert shows the initial part of the curves.

Figure 5. TGA weight loss curves of GA/clay aerogels.

Figure 6. Heat release rate as a function of time during cone calorimetry tests.

Graphical Abstract

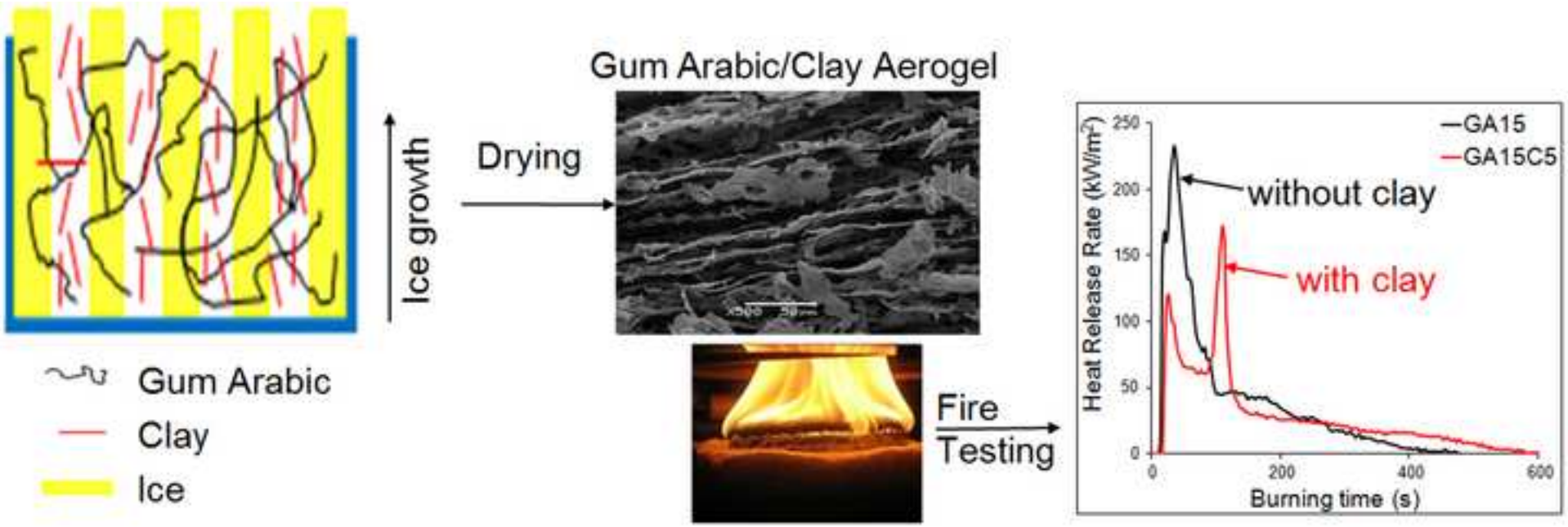

Highlights:

- “Green” gum Arabic /clay aerogels were prepared using a freeze-drying process.
- The unique solvent used in the preparation process was water.
- Gum Arabic aerogels exhibit a lamellar structure created by the ice template.
- The thermal stability and flame retardancy were improved by clay addition.

Figure 1

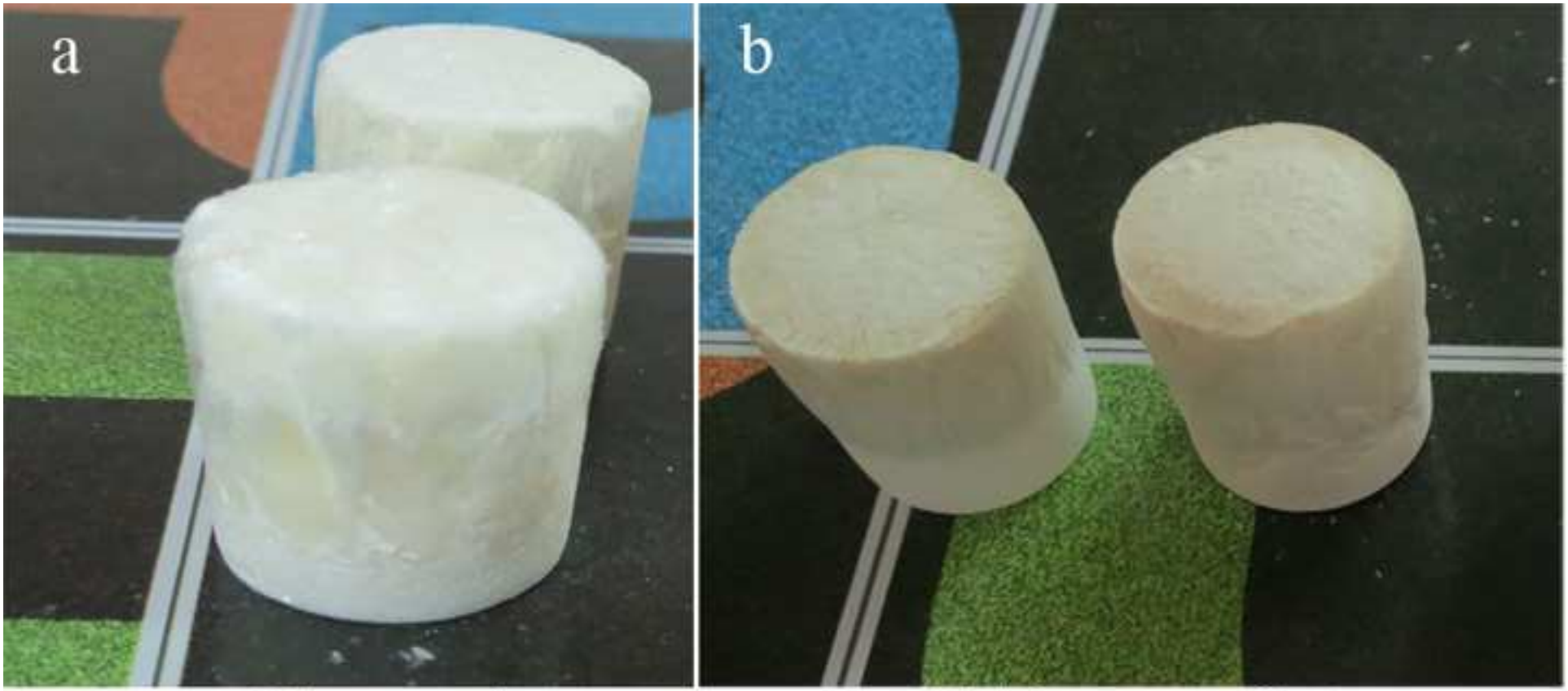

Figure 2a

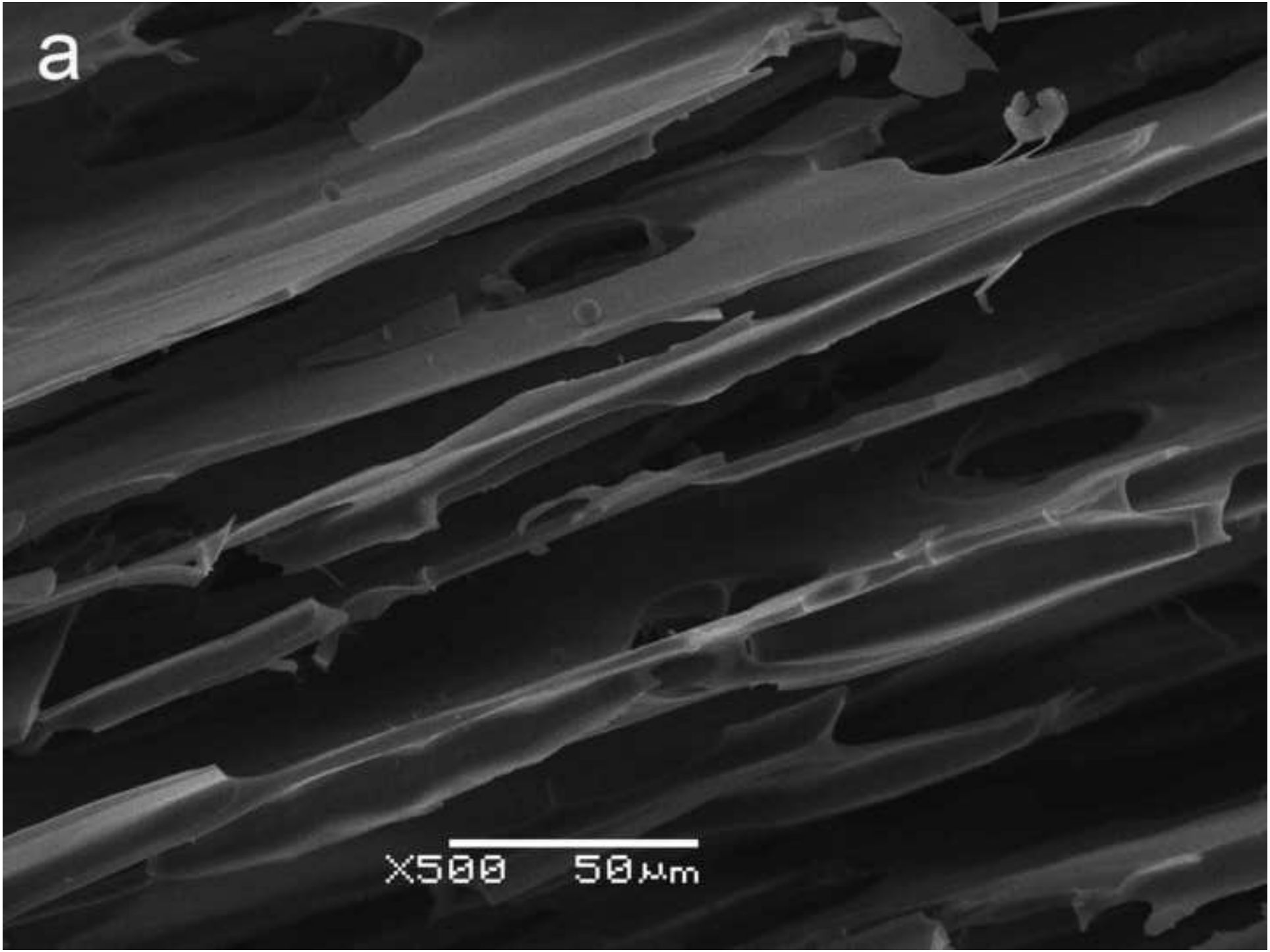

Figure 2b

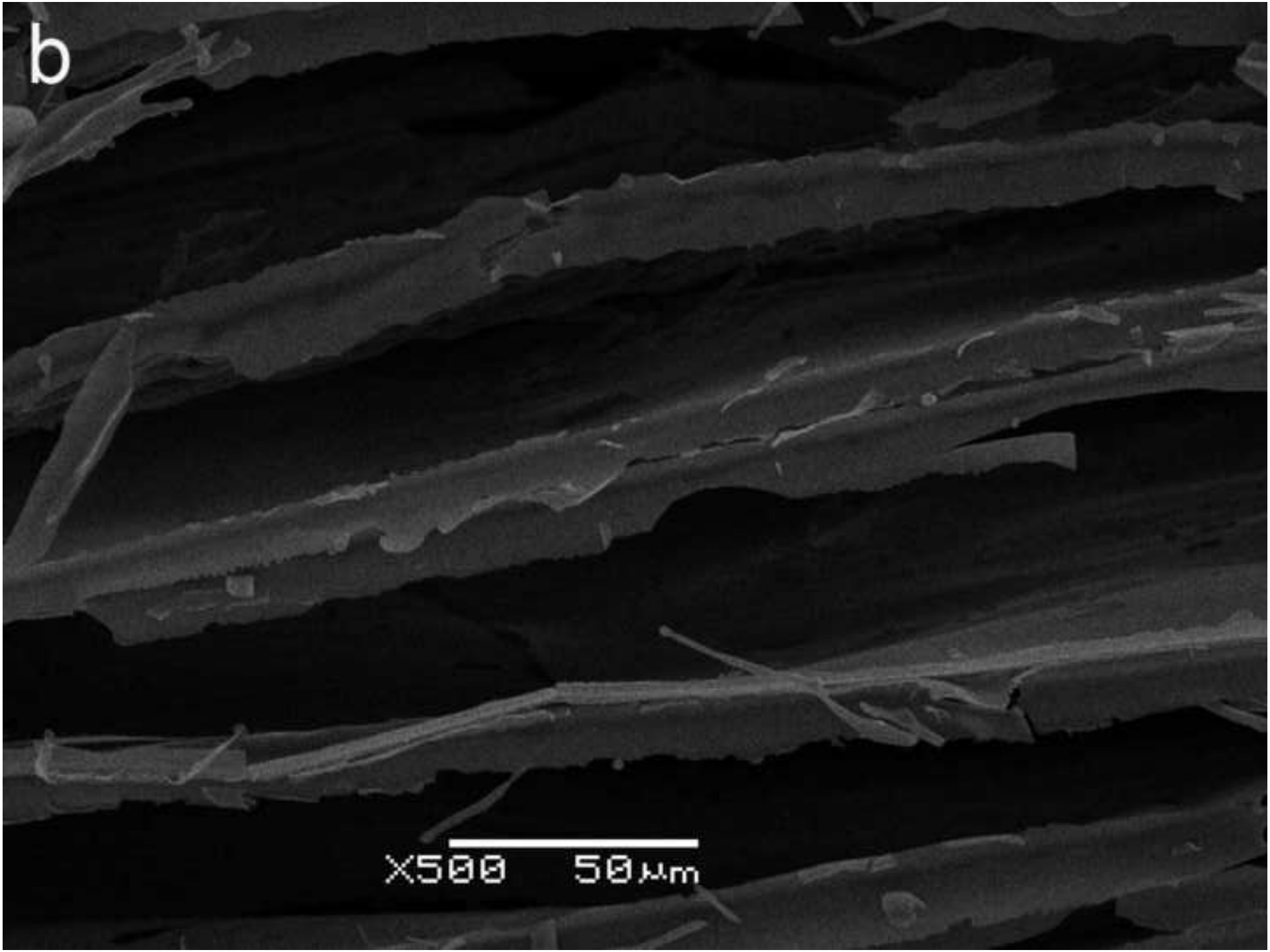

Figure 2c

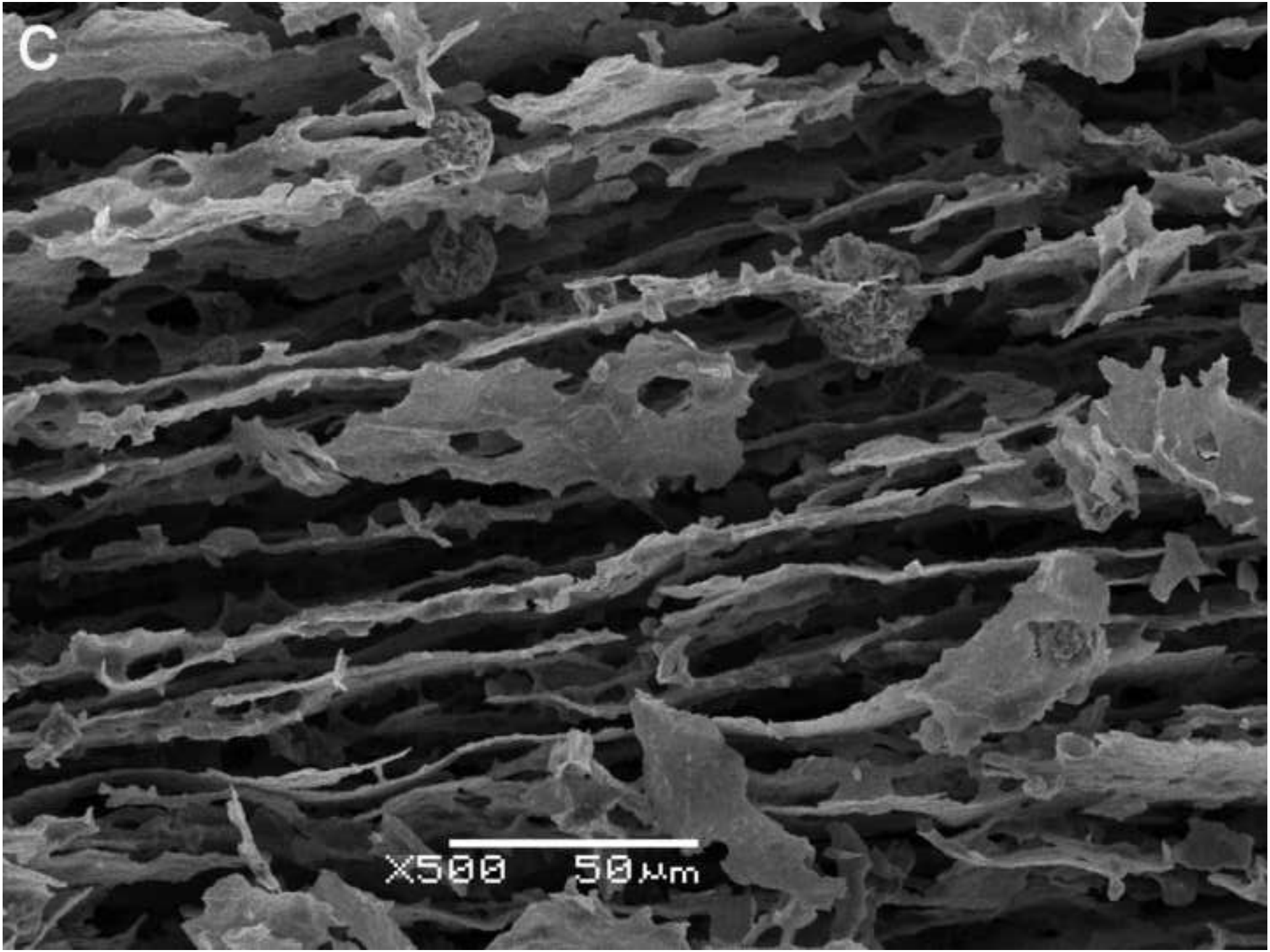

Figure 2d

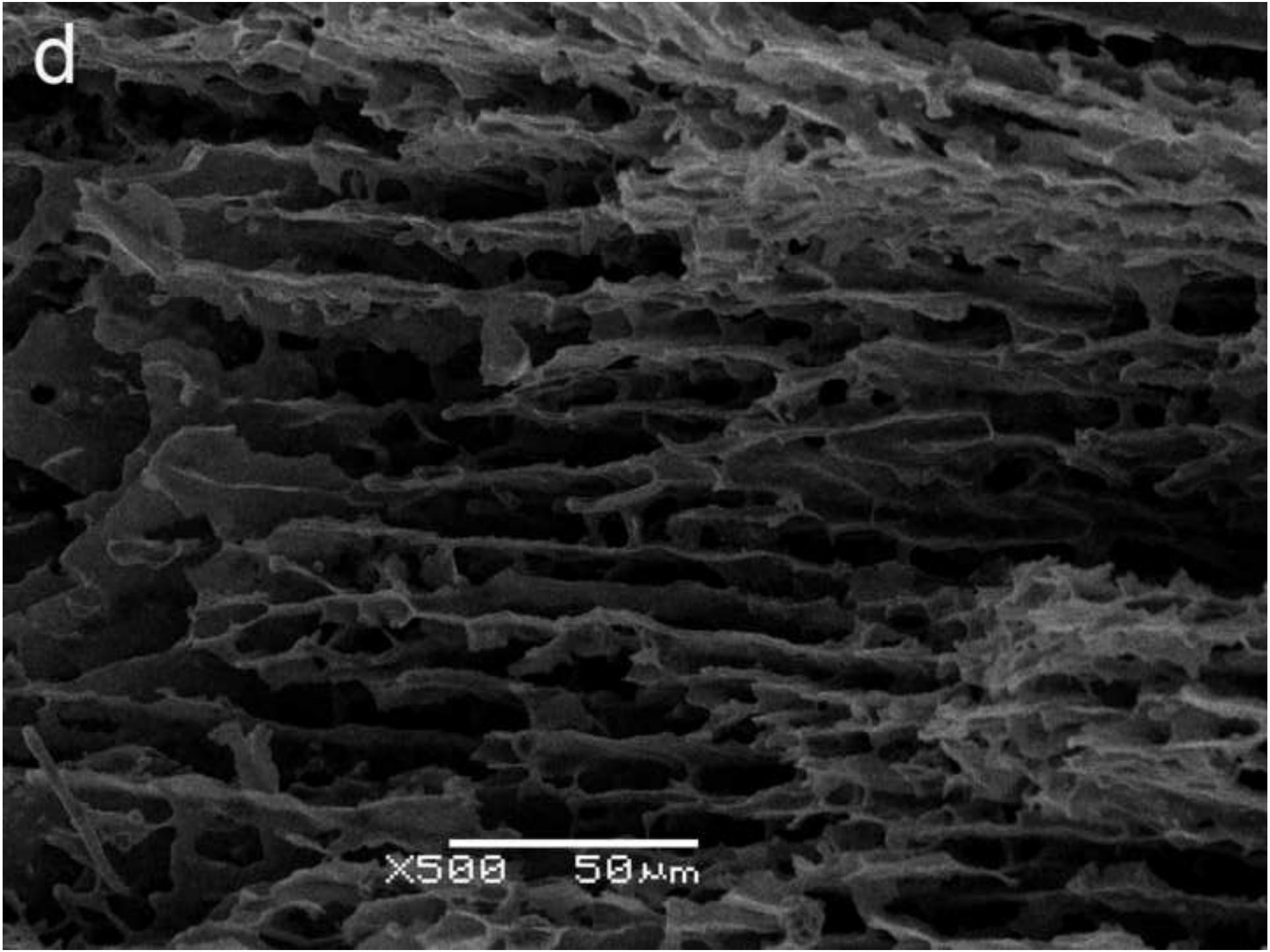

Figure 3

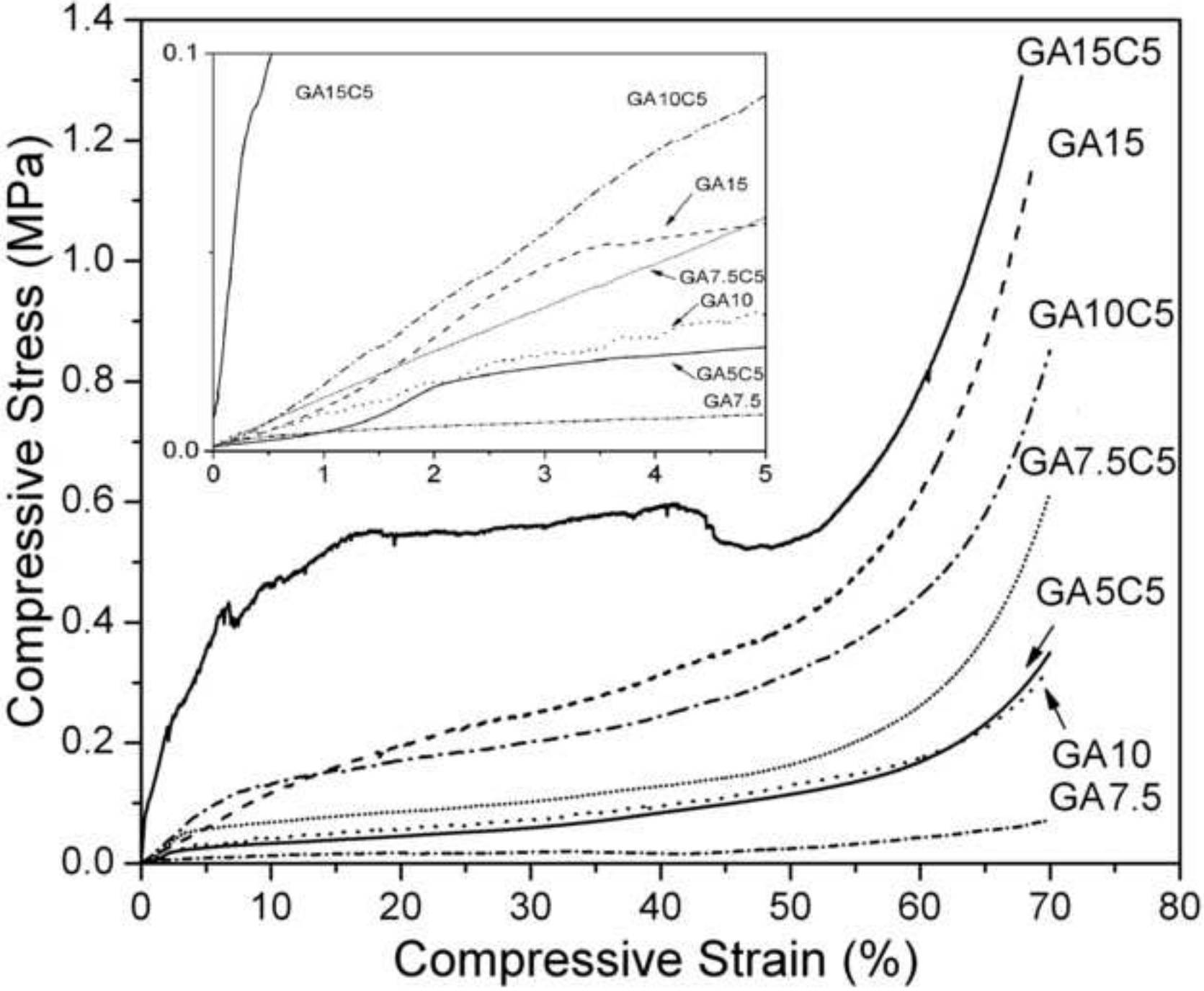
Compressive Stress (MPa)
Compressive Strain (%)
GA15C5
GA15
GA10C5
GA7.5C5
GA5C5
GA10
GA7.5
0.0
0.2
0.4
0.6
0.8
1.0
1.2
1.4
0
10
20
30
40
50
60
70
80
0.1
0.0
0
1
2
3
4
5

Figure 4

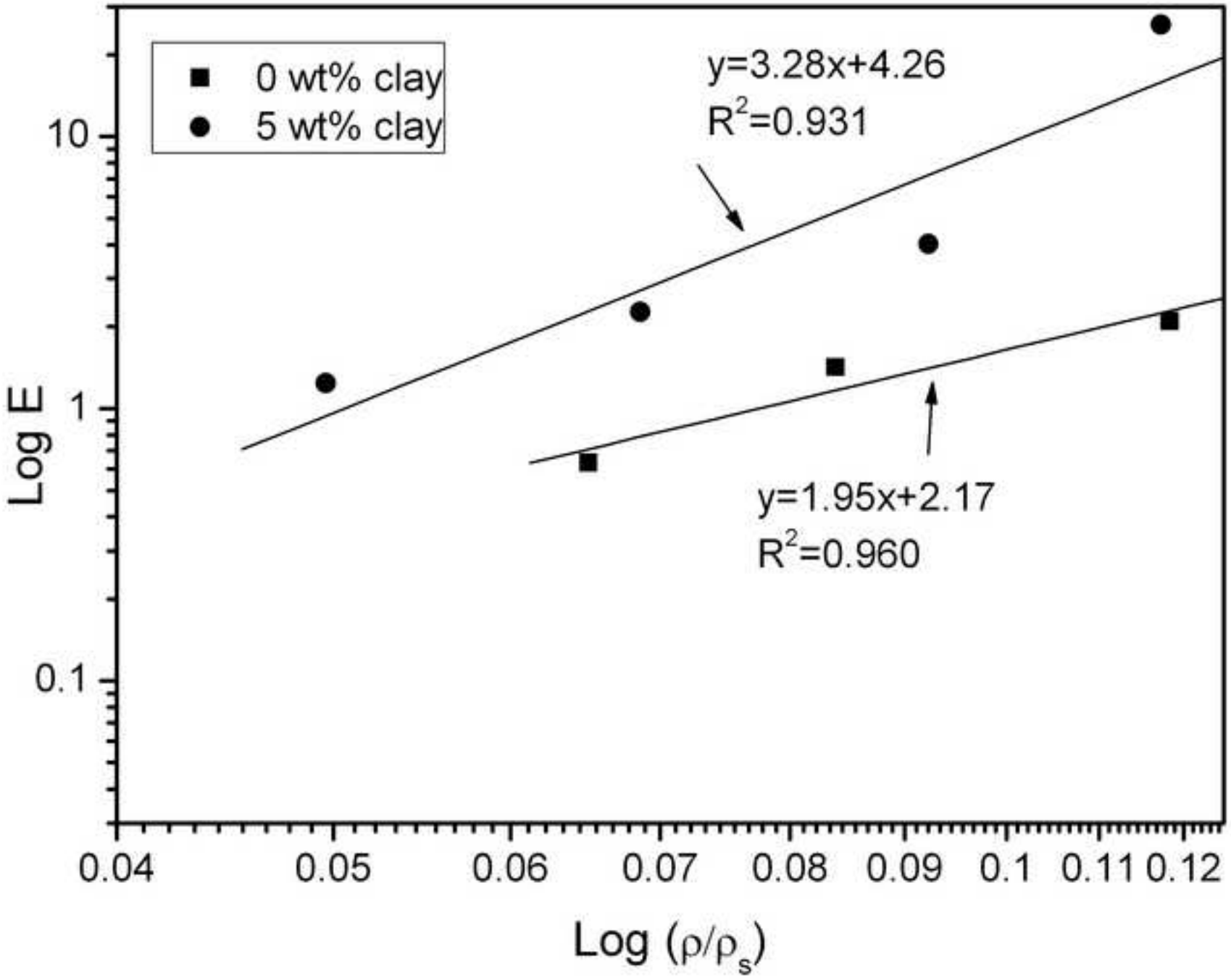
0 wt% clay
5 wt% clay
y=3.28x+4.26
R2=0.931
y=1.95x+2.17
R2=0.960
Log E
10
1
0.1
0.04
0.05
0.06
0.07
0.08
0.09
0.1
0.11
0.12
Log (ρ/ρs)

Figure 5

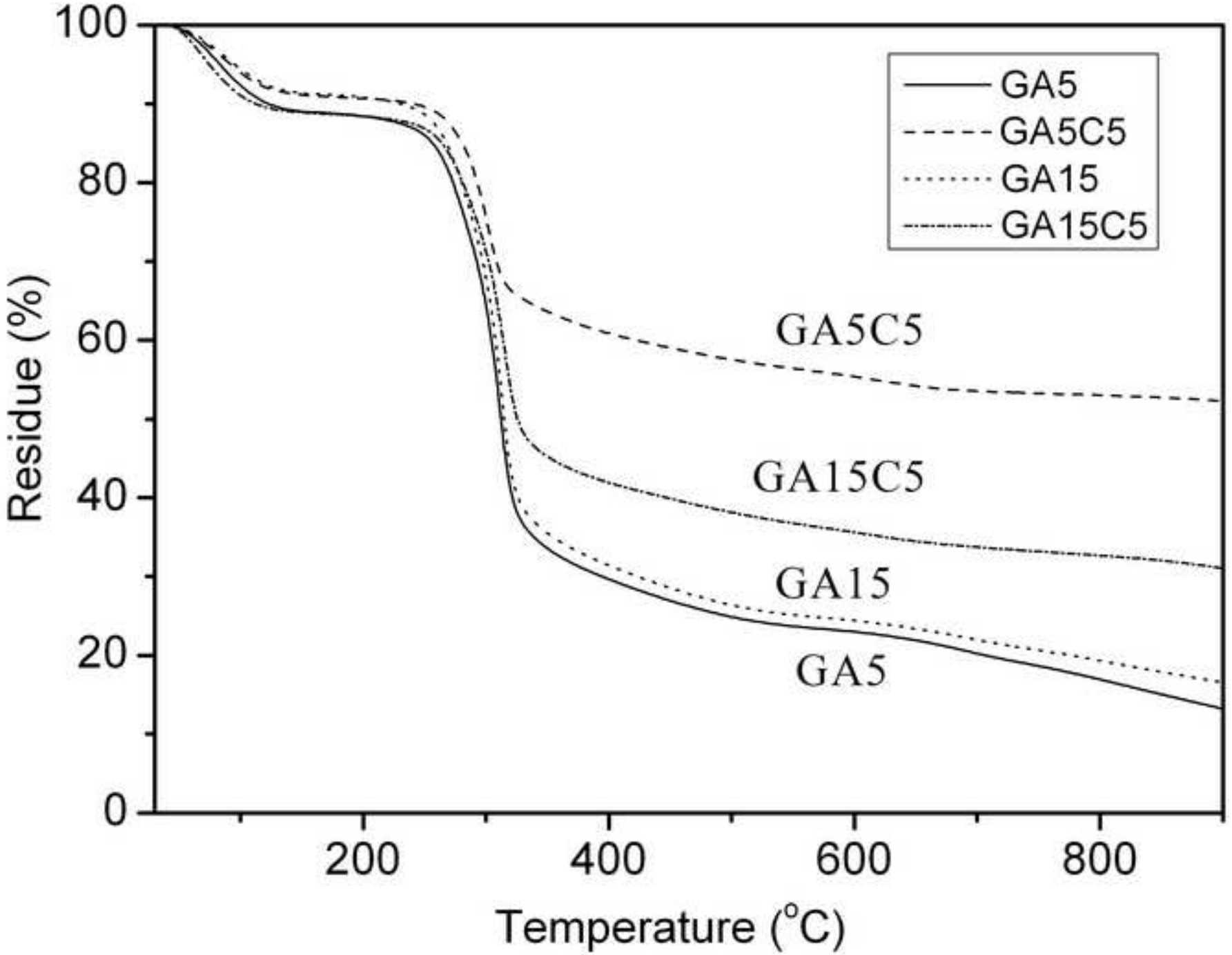
100
80
60
40
20
0
Residue (%)
200
400
600
800
Temperature (°C)
GA5
GA5C5
GA15
GA15C5
GA5C5
GA15C5
GA15
GA5

Figure 6

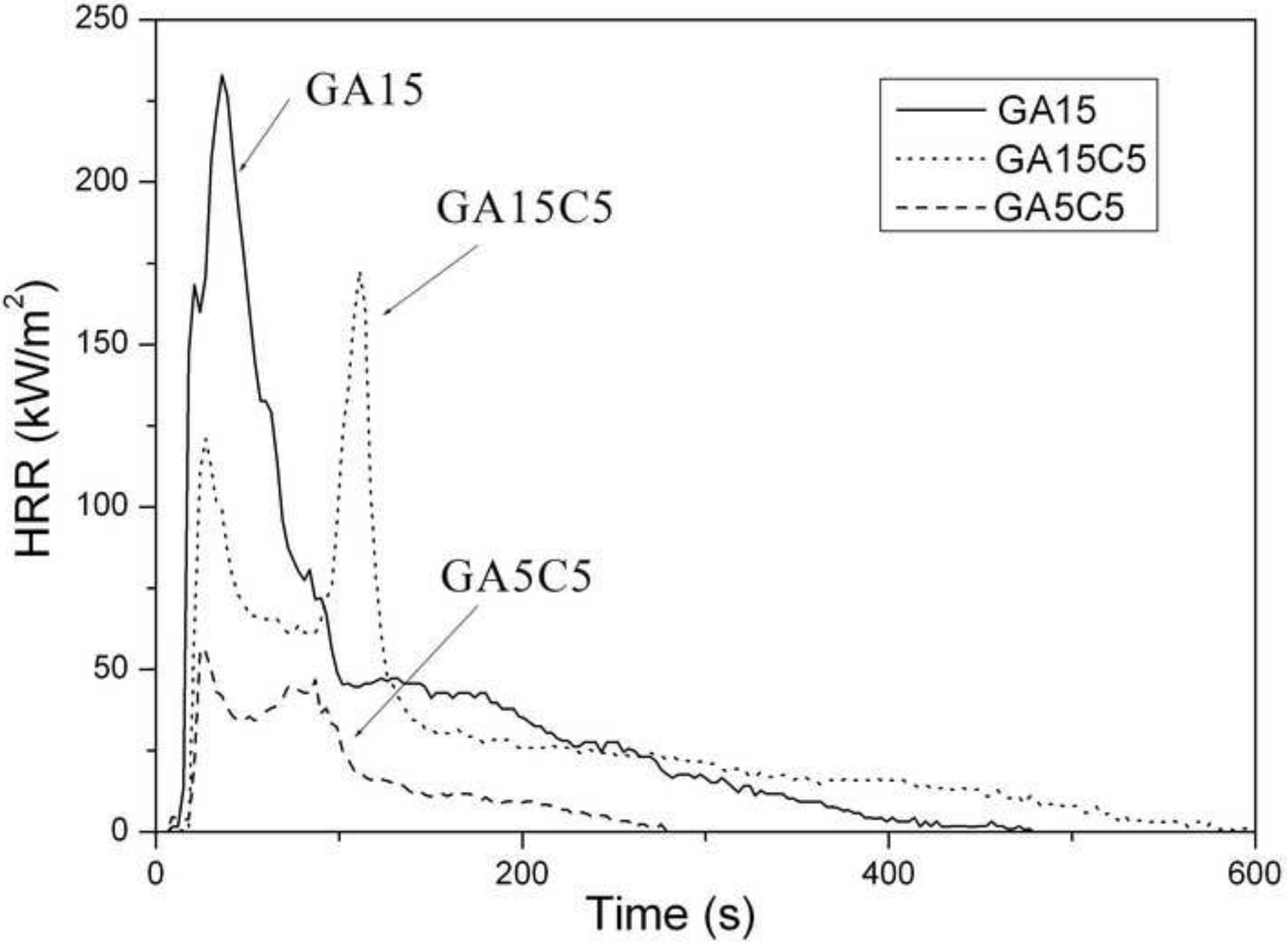
250
200
150
100
50
0
0
200
400
600
HRR (kW/m^2)
Time (s)
GA15
GA15C5
GA5C5
GA15
GA15C5
GA5C5